Available online at www.sciencedirect.com
SCIENCE DIRECT®
ELSEVIER
Journal of Nuclear Materials 329–333 (2004) 328–332
journal of nuclear materials
www.elsevier.com/locate/jnucmat

Creep deformation of iron strengthened by MX type particles

M. Tamura [a,*], H. Sakasegawa [b], A. Kohyama [c], H. Esaka [a], K. Shinozuka [a]

[a] Department of Materials Science and Engineering, National Defense Academy, 1-10-20 Hashirimizu, Yokosuka 2398686, Japan
[b] Graduate School of Kyoto University, Uji 6110011, Japan
[c] Institute of Advanced Energy, Kyoto University, Uji 6110011, Japan

Abstract

Creep deformation of bcc iron strengthened by TaN or TaC (hereinafter MX) at about 650 °C has been studied. Nano-scaled MX particles significantly lower minimum creep rate of bcc iron and retard the onset of macroscopic accelerating creep. Shrinkage during creep was observed in Ta and C containing steel. Rupture data indicate that the addition of 0.1% Ta with sufficient N is adequate for high creep resistance. However, TaC particles are stable even under applied stress as compared with TaN. In comparison, TaN particles easily grow under stress, so that TaC containing steels may provide engineering improvements under low stress.

1. Introduction

It is well known that small precipitate particles of strong carbo-nitride formers markedly increase creep rupture strength of ferritic heat resistant steel at elevated temperatures [1,2]. Reduced activation materials (RAM) are required both to reduce induced activity and to increase high temperature strength. Therefore, because nitrogen produces long lived radioactivity, candidate materials for the first wall of TOKAMAK reactors, for example F-82H, are designed to lower nitrogen as low as possible, so that strengthening is caused by (TaV)C, and other carbides [3,4]. On the other hand, since nitrogen is effective to increase high temperature strength [5], RAM containing a small amount of N have also been studied [6]. In this case, the alloy is strengthened by (TaV)(CN). However, these carbo-nitrides are called simply MX and the difference in the role of carbon and nitrogen in MX has not been studied intensively. In a previous paper we have reported that, the slope of stress vs. logarithm of time to rupture relation at 650 °C for iron containing 0.1% TaN is low as compared with that of conventional high Cr heat resistant steel, F-82H, and, therefore, a new alloy strengthened by MX is feasible [7]. In this paper, in order to clarify the difference in the role of carbide and nitride of an MX type, the basic effects of MX particles on creep in bcc iron have been studied.

2. Experiment

Model steels were melted in a vacuum furnace and hot-rolled to 12 mm thickness. The chemical compositions are listed in Table 1. The steels are designed to contain 0.05%, 0.1% and 0.2% Ta, respectively, and also contain C or N, the value of which is stoichiometric to 0.2% Ta. The steels were normalized at 1200 °C followed by pre-aging at 650 °C for 500 h in order to stabilize the microstructure at this temperature. Creep rupture tests were performed at around 650 °C under a constant load in atmosphere. Vickers hardness tests were made using a 2 kg load and precipitate particles were observed using a field emission type scanning electron microscope (FE-SEM: Hitachi S-4300).

3. Experimental results

3.1. Metallurgical observation

Vickers hardness values for the model steels are shown in Table 1. After normalizing, hardness increases, depending on the content of Ta, N or C. By pre-aging at

* Corresponding author. Tel.: +81-46 841 3811x3650; fax: +81-46 844 5910.
E-mail address: mtamura@nda.ac.jp (M. Tamura).

0022-3115/$ - see front matter
doi:10.1016/j.jnucmat.2004.04.046

Table 1
Chemical composition and summary of the test results

Alloy	Chemical composition (%)					Hardness, HV2				Rupture time (h)	Estimated rupture strength (MPa) 650 °C 100 h
						Before test		After rupture			
	C	Si	Mn	Ta	N	Norm	Pre-aging	Grip	Gauge		
FE	0.0031	0.008	0.076		0.0019	66	66	63		200	19.1
5TAN	0.0030	0.083	0.082	0.056	0.0130	151	83				68.4
10TAN	0.0028	0.008	0.074	0.093	0.0130	161	99	100	101	229	72.3
20TAN	0.0032	0.085	0.082	0.220	0.0134	197	116	97		193	74.5
5TAC	0.0150	0.082	0.081	0.050	0.0028	113	73				52.3
10TAC	0.0140	0.083	0.081	0.110	0.0028	143	143	110	107	310	73.3
20TAC	0.0160	0.008	0.090	0.170	0.0020	169	136	132		327	91.7

Norm: as normalized at 1200 °C (FE is normalized at 1000 °C); pre-aging: as pre-aged at 650 °C for 500 h after normalizing.

650 °C, hardness of the TAN series drops, but hardness decreases less for the TAC series. X-ray analysis on the extracted residues showed that cubic MX was identified in both the TAC and TAN series steels as a major compound and hexagonal MX was also found for both series steels as a minor compound. Grain size of the model steels is ranged between 100 and 150 μm.

3.2. Creep curve

Fig. 1 shows typical creep curves for FE, 10TAN and 10TAC at 650 °C. FE shows transient creep up to about 0.05% (including elastic strain) followed by accelerating creep with a moderate creep rate to rupture. The specimen was ruptured with relatively high values of rupture elongation (50%) and reduction of area (55%), though the values are strongly affected by oxidation.

Creep curves of 10TAN and 10TAC show that the addition of MX significantly lowers creep rates after a small strain for transient creep. In 10TAC negative creep was clearly observed. Even after the minimum creep rate or minimum creep strain, after the negative creep strain of the MX containing steels was held at considerably low levels up to rupture life and after about 1% strain, creep rates accelerated rapidly. 10TAN shown in Fig. 1 ruptured with elongation of 18% and reduction of area of 55%. This trend of low rupture elongation and high reduction of area is rather similar with that of martensitic heat resistant steel. On the contrary, 10TAC in Fig. 1 shows less rupture elongation (9%) and smaller necking (reduction of area of 25%) and the rupture appearance of 10TAC showed limited ductility. The average rupture elongation for the TAN series is 17% with about 60% reduction of area, and the average rupture elongation for 5TAC and 10TAC is less than that for TAN, about 8%, and reduction of area for 5TAC and 10TAC is 25% and 14%, respectively. However, 20TAC fractured along grain boundaries and rupture elongation was extremely low, i.e. less than 1% [7].

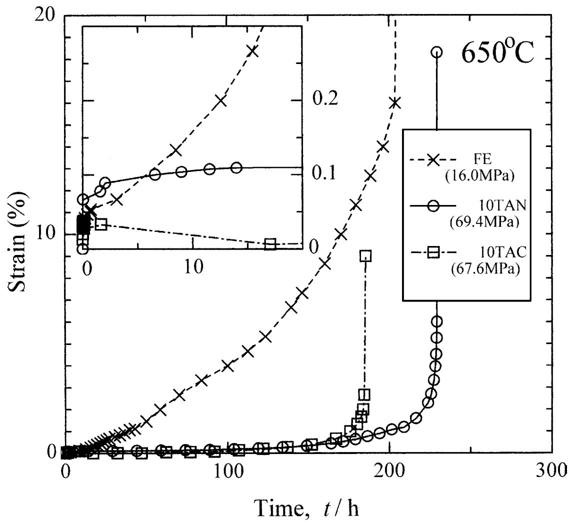

Fig. 1. Typical creep curves of FE, 10TAN and 10TAC at 650 °C.

Characteristics of the creep curve for FE are affected little by both test temperature (635–665 °C) and stress (14–29 MPa). Creep curves at 635–665 °C for the TAN series resembled those shown in Fig. 1, except that shrinkage after a small amount of transient creep strain was observed in 10TAN at 650 °C and under a low stress level of 60.7 MPa. On the other hand, shrinkage as shown in Fig. 1 was observed in 5TAC at 665 °C (41.6 MPa) and 635 °C (48.5 MPa), and, moreover, shrinkage was often observed in most of the 10TaC and 20TAC series at 650 and 680 °C.

3.3. Creep rupture test

The results of creep rupture tests at 650 °C are shown in Fig. 2. All rupture data at around 650 °C for each steel were fitted by an exponential equation [8]. It is found from Fig. 2 that the addition of MX to pure iron (FE) greatly increases rupture strength, but the time dependence of rupture strength for the TAC series steels, $|\Delta\sigma/\Delta \log t_r|$, is larger than those of the TAN series steels.

3.4. Microstructure under FE-SEM

Fig. 3 shows the back-scattered FE-SEM images of the etched surfaces of 10TAN, 20TAN and 10TAC. Precipitates of 10TAN before creep test are cuboidal and are distributed uniformly with average diameter ranging from 10 to 75 nm (Fig. 3(a)). After creep testing, large precipitates are noticeable in a grip section with average diameter ranging from 10 to 120 nm (Fig. 3(b)). In a gauge section, average diameter ranged from 10 to 94 nm (Fig. 3(c)).

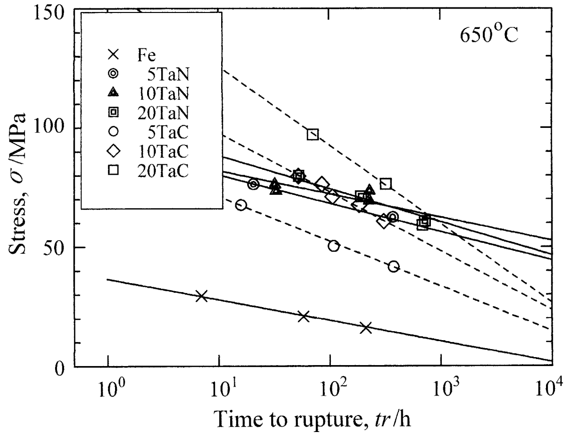

Fig. 2. Time to rupture vs. stress relation of the model steels at 650 °C.

Precipitates in 20TAN before creep testing (Fig. 3(d)) differ from those of 10TAN in size and shape. Besides fine cuboidal particles of about 10 nm, coarse rod type precipitates 35 nm in diameter and 90–190 nm in length are found. After creep testing, besides the fine precipitates of about 10, 40 nm cuboidal particles and large rod type particles with about 250 nm long are found (Fig. 3(e)). Also, needle typed precipitates as long as 600 nm were found in a grip section of a crept 20TAN sample. Particles which appear white in Fig. 3 contain Ta. Extracted residues of the grip portion of 20TAN were examined by XRD and strong diffraction peaks of cubic TaN, hexagonal TaN and FeO were identified. FeO may come from the surface oxide layer of a screw. However, it is not possible to correlate the morphology of the precipitates shown in Fig. 3(e) with the crystal structure of TaN.

In 10TAC, very fine precipitates of about 5 nm or less were observed before creep testing (Fig. 3(f)). In a grip section of a creep-ruptured specimen, both fine cuboidal precipitates and rather coarse rod or plate like precipitates were observed (Fig. 3(g)). The average size ranged from 6 to 40 nm. The size distribution and number density of the precipitates in the gauge portion was similar with that of a grip portion (Fig. 3(h)).

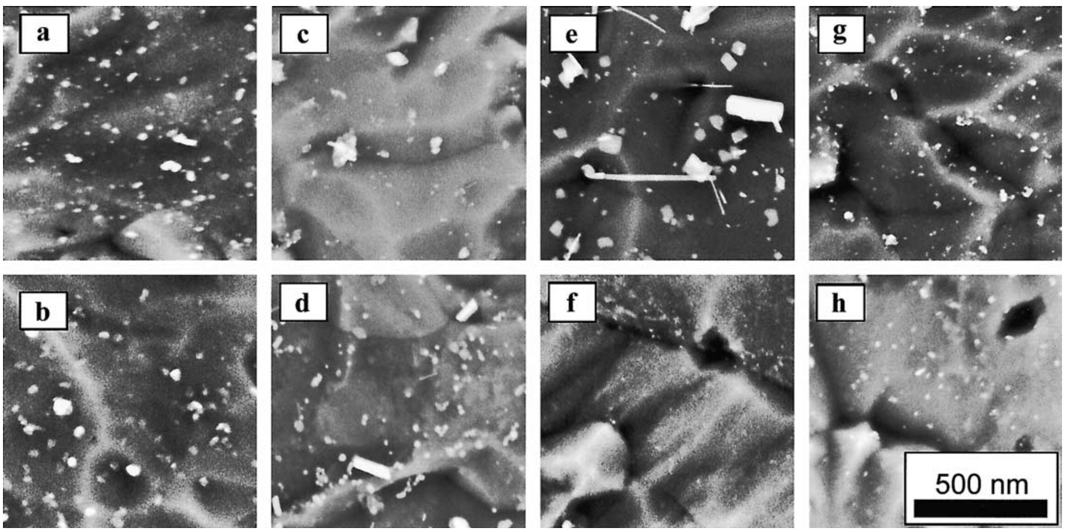

Fig. 3. FE-SEM back-scattered images of 10TAN, 20TAN and 10TAC. 10TAN was tested under 73.5 MPa, $t_r = 229$ h [(a) before test, (b) grip and (c) gauge]. 20TAN was tested under 71.1 MPa, $t_r = 193$ h [(d) before test and (e) grip]. 10TAC was tested under 60.7 MPa, $t_r = 310$ h [(f) before test, (g) grip and (h) gauge].

4. Discussion

4.1. Precipitation behavior

Hardness of the model steel after creep test was given in Table 1. Rupture time of the creep test is shown in Table 1. If Ta is fully dissolved in a normalized state, the difference in hardness between the FE and TAN series should be explained by solid solution hardening of Ta and N. And the difference in hardness between the FE and TAN series before and after creep test should be explained by precipitation hardening due to fine precipitates in TAN, if soluble N and Ta in bcc iron is negligibly small at 650 °C [4] and if the hardening effect due to creep strain in a grip portion can be neglected, because stress in a grip portion is 25% or less of that of a gauge portion. The hardness in 20TAN clearly decreases during the creep test, though not for the case of 10TAN. These results are consistent with the morphology of TaN particles shown in Fig. 3, where the stability in particle size and coarsening of TaN in creep-ruptured specimens of 10TAN and 20TAN are shown.

On the other hand, the hardness of the TAC series is higher than for those of the TAN series as shown in Table 1, when Ta content is higher than 0.1%. Hardness of 10TAC decreases greatly due to creep, which should correspond to the coarsening of precipitates as demonstrated in Fig. 3(f)–(h). Hardness numbers for 10TAC were identical for grip and gauge portions, due to similar size distributions of TaC. The hardness of 20TAC did not decrease during the creep test.

It is demonstrated from Fig. 3 that TaC is difficult to precipitate and grow in a bcc matrix as compared with TaN. Also, growth of MX appears to be accelerated by creep, because, as shown in Fig. 3(d) and (e), the maximum sizes of MX after the creep test of about only 200 h are much larger than those from before the creep test, which under goes stress free aging for 500 h. It is reasonable to consider that enough stress to generate dislocations acts on the grip portion, though the stress is low. MX is easy to nucleate on dislocations and dislocations strongly aid the growth of MX [9,10]. Therefore, the growth of MX during creep testing as shown in Fig. 3 can be explained by the presence of dislocations generated in the specimen.

Precipitates of 10TAN and 20TAC were observed using a transmission electron microscope (TEM) and the results were reported in the previous paper [7]. The size of MX measured in TEM is the same as that of FE-SEM and, therefore, the results shown in Fig. 3 are confirmed. From the above discussion it is concluded that precipitated TaC particles in a bcc matrix are more stable compared with TaN independent of the presence of stress and within the TAN series steels, precipitates in 10TAN are more stable than 20TAN.

4.2. Creep strength

Rupture strengths at 650 °C and 100 h are calculated using regression equations of the exponential type [8] and the results are shown in Table 1. The rupture strength at 100 h increases with increase in Ta content and the increasing rate, $\Delta\sigma/\Delta\mathrm{Ta}$, of TAC series steel at around 0.1% Ta is larger than that of the TAN series.

Combining the estimated rupture strength with the knowledge that $|\Delta\sigma/\Delta\log t_r|$ of the TAN series is smaller than that of TAC series, ductility of the TAN series is higher than that of the TAC series [7], and the microstructure of 10TAN is more stable compared with 20TAN (Fig. 3), it is concluded phenomenologically that the addition of 0.1% Ta with sufficient amount of N in bcc iron is suitable for the basic design of a structural material with high creep resistance. However, to apply this concept to practical material, many engineering problems should be solved. One of the problems is the abnormal growth of TaN particles shown in Fig. 3(d) and (e). This phenomenon was observed only in a steel containing 0.2% Ta. However, an intrinsic character of TaN in the matrix may cause the abnormal growth of TaN. Therefore, careful attention is necessary for the practical application of this alloy.

The time dependence of rupture strength of the TAC series is large, due to precipitation and growth of TaC during creep. This fact and the hardness change shown in Table 1 imply that solid solution hardening might be effective even at 650 °C but the effect disappears within a very short time, and strength at 650 °C over long times is actually supported by precipitate particles. Incidentally, particle sizes in the TAC series remains very fine even after creep testing and smaller than that for the TAN series. Therefore, TaC containing steel is applicable as a structural material, though improvement in ductility is necessary.

5. Conclusion

Creep deformation at 650 °C over about 300 h has been studied on bcc iron strengthened by nano-scaled TaN or TaC particles. Distribution of the particles was observed under FE-SEM and following conclusions were obtained.

(1) The addition of 0.1% Ta with sufficient amount of N is suitable for the basic design of structural material with high creep resistance.
(2) TaN is easy to precipitate and grow under either simple thermal aging or creep deformation. On the contrary, TaC precipitates and grows little only during thermal aging. However, TaC easily precipitates and grows on dislocations induced during creep, which is clearly observed as shrinkage during

primary creep. This apparently leads to the large time dependence of rupture strength of TaC containing steels and, thus, the decrease in rupture strength at long time.

(3) TaC particles are more stable than TaN, and, therefore, TaC containing steels is more promising under low stress if suitable countermeasures for shortness in ductility are adopted.

Acknowledgements

The authors thank Mr Tanaka of Nissei Science Co. for arranging to use the FE-SEM. A part of this study has been done under a support of SUZUKI foundation.

References

[1] V.K. Sikka, C.T. Ward, K.C. Thomas, in: A.K. Khare (Ed.), Ferritic Steels for High-Temperature Applications, ASM, Metals Park, OH, 1983, p. 65.

[2] S.J. Sanderson, in: A.K. Khare (Ed.), Ferritic Steels for High-Temperature Applications, ASM, Metals Park, OH, 1983, p. 85.

[3] M. Tamura, H. Hayakawa, M. Tanimura, A. Hishinuma, T. Kondo, J. Nucl. Mater. 141–143 (1986) 1067.

[4] M. Tamura, K. Shinozuka, H. Esaka, S. Sugimoto, K. Ishizawa, K. Masamura, J. Nucl. Mater. 283–287 (2000) 667.

[5] A. Iseta, Y. Sawaragi, K. Yoshikawa, Tetsu-to-Hagane 77 (1991) 582.

[6] A. Kohyama, Y. Kohno, M. Kuroda, A. Kimura, F. Wan, J. Nucl. Mater. 258–263 (1998) 1319.

[7] M. Tamura, H. Sakasegawa, A. Kohyama, H. Esaka, K. Shinozuka, J. Nucl. Mater. 321 (2003) 288.

[8] M. Tamura, H. Esaka, K. Shinozuka, ISIJ Int. 39 (1999) 380.

[9] Y. Kadoya, E. Shimizu, Tetsu-to-Hagane 85 (1999) 827.

[10] K. Shinozuka, M. Tamura, H. Esaka, Tetsu-to-Hagane 88 (2002) 100.